Article

10-Port MIMO Inverted-F Antenna for LTE Bands 42/43/48/49 Bands Smartphone Applications

Muhammad Zahid * , Aliya Khalid , Hira Moazzam , Hajra Sadaqat , Sultan Shoaib , Yasar Amin

Posted Date: 29 August 2023

doi: 10.20944/preprints202306.0073.v2

Keywords: antenna for handset; m-MIMO; sub-6 GHz; LTE bands 42/43/48/49; future generation

Article

10-Port MIMO Inverted-F Antenna for LTE Bands 42/43/48/49 Bands Smartphone Applications

Muhammad Zahid [1,*], Aliya Khalid [1], Hira Moazzam [1], Hajra Sadaqat [1], Sultan Shoaib [2], and Yasar Amin [1]

[1] Department of Telecommunication Engineering, University of Engineering and Technology, Taxila, 47050, Rawalpindi, Punjab, Pakistan
[2] School of Applied Science Computing & Engineering, Wrexham Glyndwr University, Wales, United Kingdom
* Correspondence: muhammad.zahid@uettaxila.edu.pk

Abstract: This paper presents a design and performance analysis of a 10-element 5G massive MIMO antenna array for sub-6GHz mobile handsets, specifically for LTE bands 42 (3400-3600 MHz), 43 (3600-3800 MHz), 48/49 (3550-3700 MHz) applications. The proposed antenna array consists of 10 closely spaced linearly polarized inverted-F antennas with a compact size of $20 \times 9\ mm^2$ of a single element. The proposed antenna array provides high gain, high efficiency, and low correlation between the antenna elements, which results in improved channel capacity, increased data rate, and enhanced signal quality. The performance of the antenna array is evaluated in terms of the radiation pattern, gain, efficiency, and correlation coefficient. The simulation and measured results show that the proposed antenna array achieves an approximate peak gain of 3.1 dBi at the resonance frequency, a total efficiency of 65 %, and a low correlation coefficient of 0.06 between the antenna elements. Therefore, the proposed 5G massive MIMO antenna array is a promising candidate for sub-6 GHz mobile handsets, particularly for LTE bands 42/43/48/49 applications.

Keywords: antenna for handset; m-MIMO; sub-6 GHz; LTE bands 42/43/48/49; future generation

1. Introduction

The demand for faster data speeds, lower latency, and better coverage has increased as a result of the quick development of mobile communication services. Massive multiple-input multiple-output (MIMO) antenna arrays are projected to be used in fifth-generation (5G) wireless networks to meet these requirements because they can considerably boost the system's capacity and spectral efficiency. Massive MIMO antenna arrays are difficult to integrate into mobile phones due to space constraints, and intricate antenna design. Small, multi-standard compliant antenna systems that support a wide range of wireless protocols would be very useful for future portable gadgets. Multiple-input multiple-output (MIMO) aerial technology has become essential for the development of portable devices because of its ability to increase data throughput without increasing the power and bandwidth [1].

Due to their success without requiring more power or better spectrum efficiency, MIMO LONG-TERM EVOLUTION (LTE) systems have attracted a lot of attention. In a situation with severe fading, a multiple antenna system can often be used in MIMO mode or diversity mode [2]. There is currently a need for antennas with a wider bandwidth compact MIMO aerial with excellent isolation for 5G applications as a direct result of the development of new technologies and applications [3]. The next generation of high-bit-rate wireless communications will benefit from MIMO RF systems reduced multipath fading and increased channel capacity. Although important for the tiny size of today's mobile designs, the physical structure must also effectively utilize the available space for these future ideas [4]. Due to the limited space allotted for smartphone antennas, it is technically difficult to construct a massive MIMO antenna system with less return loss or coupling [5].

In the latest research, many decoupling methods have been presented to enhance isolation for the MIMO system, including, parasitic element [6], the neutralization line (NL) method [7], etching

Preprints (www.preprints.org) | NOT PEER-REVIEWED | Posted: 29 August 2023 doi:10.20944/preprints202306.0073.v2

slot technique [8], decoupling of ground branch technique [9,10] structures of metamaterial [11], and decoupling networks [12]. Several strategies have been proposed by researchers to limit mutual coupling between the radiators, including the use of a defective ground plane [13], structures with electromagnetic bandgap [14], and a perpendicular feeding network [15]. In order to achieve effective isolation, parasitic F-shaped stubs were utilized in [16] between the radiating patches. For the minimization of mutual coupling, a two-element MIMO aerial was equipped with an electric-LC resonator [17]. For improved isolation between the MIMO antennas, a stub followed by rectangular gaps in the ground plane was used in the design of the antenna [18]. In [19], a dual-band 8×8 antenna array is designed, in which a decoupling stub is used to reduce mutual coupling. To acquire enhanced isolation balanced antenna elements are used [20].

MIMO technology is used by LTE to increase the effectiveness of radio spectrum usage, and it is anticipated to be a crucial component of LTE networks [21]. MIMO systems were originally used in a common mobile phone network called HSDPA (High-Speed Downlink Packet Access). Shortly later, this technology was first employed as the foundation for the LTE standard [22]. The 3400-3800 MHz band, which unites LTE bands 42 (3400-3600 MHz) and 43 (3600-3800 MHz), has received recognition from many countries as a pioneer in the development of 5G massive MIMO. A decision by the European Union (EU) to prioritize the development of the 3400-3800 MHz spectrum is one example [23]. China is looking into using the sub-6GHz and 3400-3600 MHz bands for 5G [24], and Korea's decision to conduct their exploratory research in the 3400–3700 MHz band [25]. The next 5G multiband communication will require more than LTE bands 42 and 43.

The F-shaped MIMO antenna not only meets mutual coupling requirements but also those for lower size and operating frequency range in addition to WiMAX applications [26]. A planar inverted-F antenna (PIFA) with an inverted-T-shaped open-slot is introduced. The proposed PIFA operates with a wide bandwidth of 78% due to the multimode technology [27]. A defected ground structure-based F-shaped patch antenna with LC analytical modelling is presented in this work. The proposed DGS antenna is working between 3.4-3.6 GHz over -10 dB impedance bandwidth in [28]. A new design of MIMO antenna array for fifth generation (5G) mobile handsets is proposed. The configuration of the design consists of eight planar-inverted F antenna (PIFA) elements located at different corners of the smartphone printed circuit board (PCB) [29]. The proposed inverted-F Antenna is compared in table 1, which shows that the proposed antenna has high gain from the table and also high bandwidth from those whose resonance is 3.5 GHz which shows the novelty of proposed design.

Table 1. Comparison of a single Inverted F-shaped Antennas in MIMO.

Ref. No.	Dimension (mm^2)	Resonance Freq. (GHz)	Bandwidth (MHz)	Gain (dBi)
[26]	31×28	3.5	1350	4.5
[27]	15×6.2	4.5	2000	not mentioned
[28]	19.3×6.2	3.5	250	not mentioned
[29]	26×12	3.55	600	not mentioned
Proposed	20×9	3.6	700	5.1

Taking into consideration the previous analysis of the problems of MIMO antenna structures in 5G, a MIMO antenna array is presented for the upcoming 5G mobile handset applications. The proposed antenna array functions in the sub-6 GHz's 5G bands. The design of the article is arranged as follows. Section 2 clears the structure of the designed MIMO antenna array. In Section 3, the simulated results are explained and compared with measurement setup of the proposed MIMO antenna array such as antenna efficiency, radiation pattern, ECC, and S-parameter are described in detail. Section 4 brings the article to a conclusion.

Preprints (www.preprints.org) | NOT PEER-REVIEWED | Posted: 29 August 2023 doi:10.20944/preprints202306.0073.v2

2. Methodology

The front view of a single element in a ten-port massive MIMO antenna is shown in figure 1, along with its complete detailed dimensions. The compact size of each array element is $20 \times 9\ mm^2$ at 3.6 GHz, printed symmetrically on the long side of "Rogers RT/duroid 5880 (tm)". The thickness of the substrate is 0.79 mm, its dielectric constant (ϵ_r) is 2.2, and the loss tangent ($tan\delta$) is 0.0009. The main PCB has dimensions of $150 \times 70 \times 0.79\ mm^3$. The 50 Ω microstrip-line feeds are printed on the main PCB to excite the inverted-F radiator. On the back side of the substrate, two types of slots were applied, the one is ground cut with length = 10 mm to achieve a wideband (to cover LTE 42 and LTE 43), and the isolation cut with a length of 8 mm is imprinted to achieve better isolation. Additionally, in figure 1 and figure 2 the detailed dimensions of the 10×10 massive MIMO antenna are clearly mentioned inside the view. The simulation tool used for the simulation of a proposed massive MIMO antenna design was CST Microwave Studio.

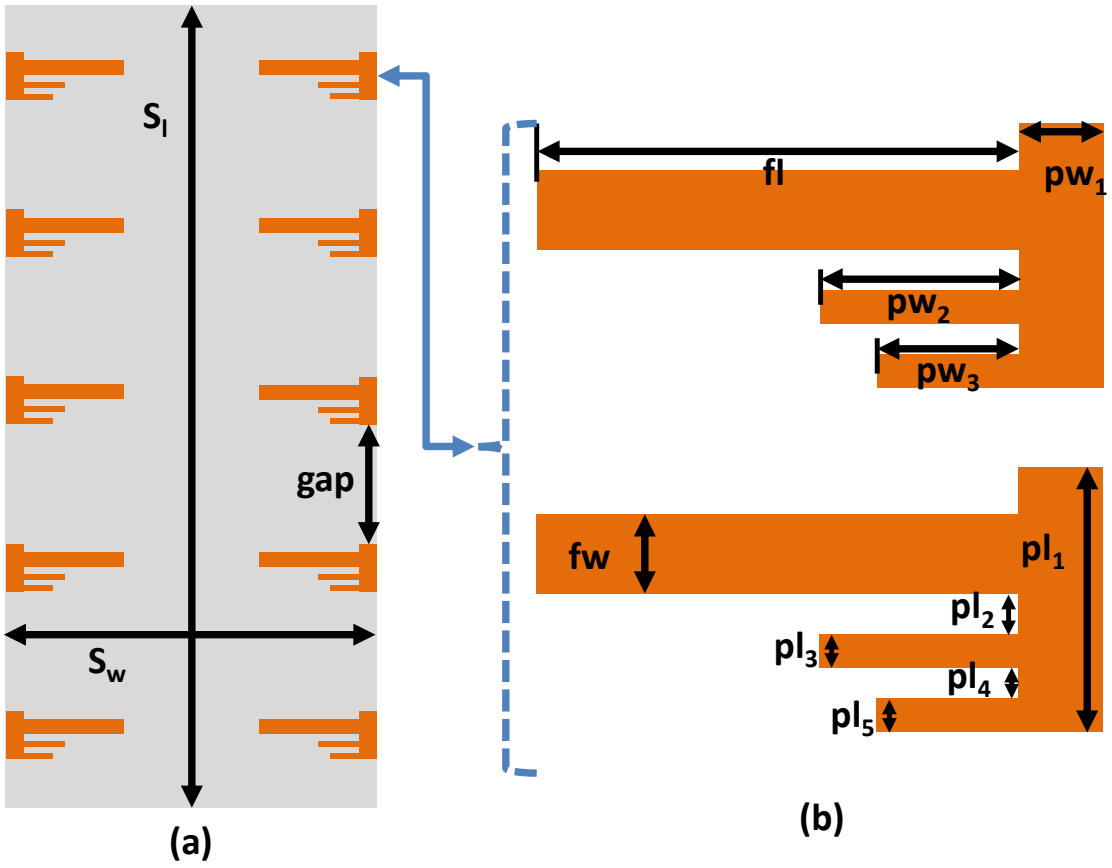

Figure 1. (a) Dimensions and geometry of front view of the proposed MIMO antenna design (b) dimensions of top layer.

The dimensions pw_1, pw_2, pw_3, pl_1, pl_2, pl_3, pl_4, and pl_5 represent the widths and lengths of patch stubs in an inverted-F antenna. And, fl, fw are the length and width of the 50Ω feedline. The dimensions gcw_1, gcw_2, gcl_1, and gcl_2 show the width and length of ground slots, whereas gap_1 and gap_2 are the separations between ground slots. A gap_3 is the distance of the topmost slot from the upper corner and gap_4 is the distance of the bottom slot from the lower corner. For better understanding, maintaining the minimum distances between each antenna will offer the most elements that's why such acceptable isolation is obtained of the 10×10 MIMO antenna. All parameters and dimensions of a planar inverted F-shaped antenna are mentioned herein from Figure 1 and figure 2 in Table 2.

Preprints (www.preprints.org) | NOT PEER-REVIEWED | Posted: 29 August 2023 doi:10.20944/preprints202306.0073.v2

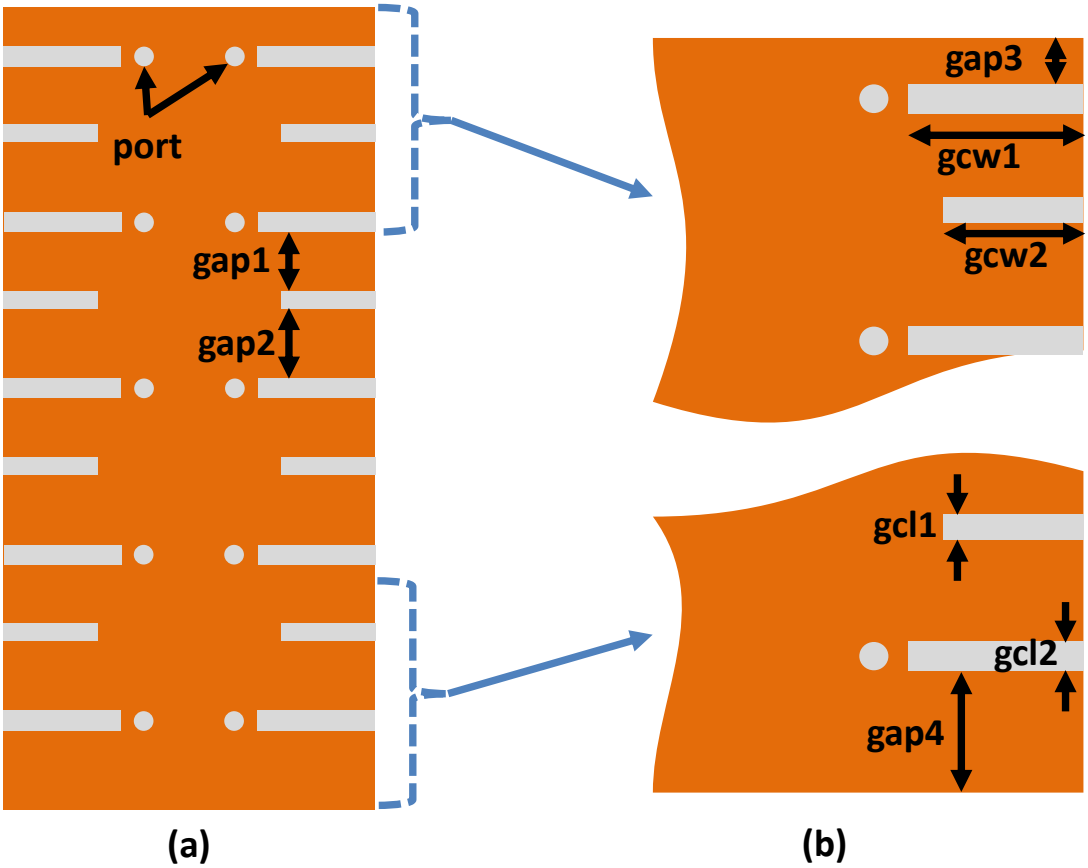

Figure 2. (a) Dimensions and geometry of back view of the proposed MIMO antenna configuration (b) dimensions of bottom layer.

Table 2. Parameters of a Proposed Antenna.

Parameter	Value (*mm*)	Parameter	Value (*mm*)	Parameter	Value (*mm*)
S_l	150	S_w	70	gap	22
fl	16.5	fw	2.43	pw_1	3.5
pw_2	7	pw_3	5	pl_1	9
pl_2	1.785	pl_3	1	pl_4	1
pl_5	1	gap1	12.8	gap2	15
gap3	9.15	gap4	15.15	gcw1	9.99
gcw2	8	gcl1	1.5	gcl_2	1.7

Figure 1 showed the magnified view of the Ant1. The F-shaped monopole element is kept farther apart so that the gap (g) between two F-shaped elements i.e., from the bottom of the inverted F-shaped to the top of it, is maintained as g = 22 *mm*. fl = 16.5*mm* and fw = 2.43*mm* are the length and width of the microstrip-line feed respectively which is printed on the main system PCB. The lowest horizontal arm of the inverted F-shaped monopole antenna has a gap pl_2 = 1.785*mm* with the feedline. The fabricated prototype is presented in figure 3.

Preprints (www.preprints.org) | NOT PEER-REVIEWED | Posted: 29 August 2023 doi:10.20944/preprints202306.0073.v2

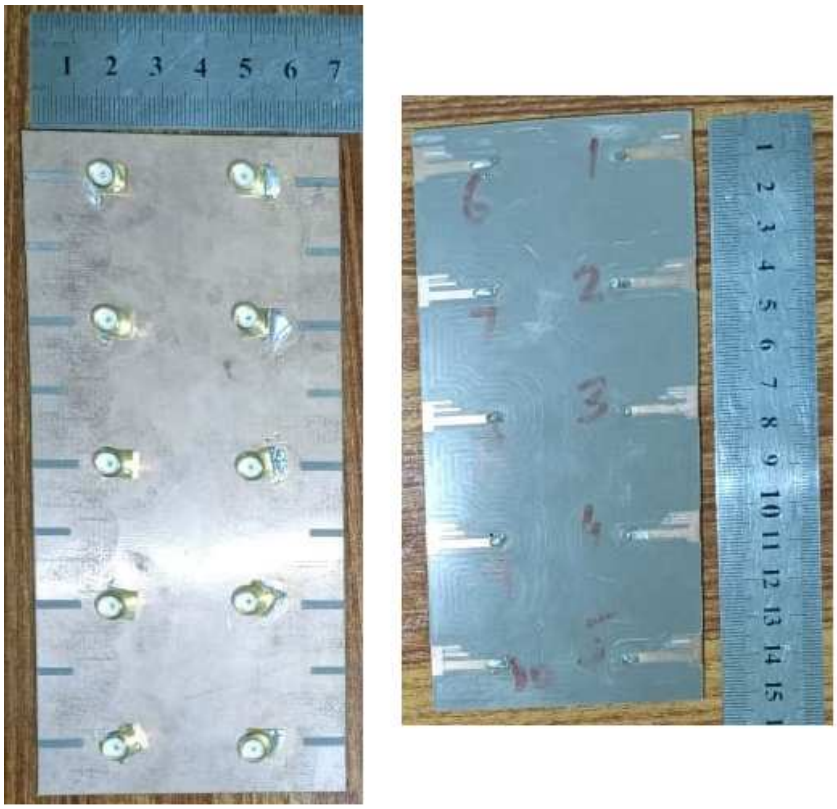

Figure 3. Fabricated prototype (a) Back view (b) Front view

3. Results and Discussions

Figure 3 shows the back and front view of the prototype, as well as the proposed 10-element 5G MIMO antenna, which has been constructed and tested. All 10-element antenna feeding points are directly coupled through the ground plane to the 50Ω SMA connectors. The next subsections detailed the measured and simulated results as well as the performance matrices of the proposed 5G MIMO antenna.

3.1. S-PARAMETERS

Figure 4 shows the measurement of s-parameters of the proposed Ant1. The graph shows that the proposed Ant1's reflection coefficient is better than -6 dB (VSWR 3:1). The simulated and measured results of Ant1 have shown desirable fractional bandwidths of 19.97% (3380 - 4130 MHz) which covers the LTE bands, such as LTE 42, LTE 43 and LTE 48/49 respectively. It is supposed to discuss the simulated and measured results of the first five antennas that are on the right side as mentioned in figure 3, except the ECC and radiation pattern.

The simulated results of the designed MIMO antenna array from antenna 1 to antenna 5 as in the sequence of figure 3 are depicted in figure 5. From figure 5, the simulated reflection coefficients are shifted to a higher frequency of around 100 MHz. According to analysis, the reflection coefficient is significantly better than -6 dB for all operational bands (3:1 VSWR, voltage standing wave ratio) and covers LTE bands 42, 43, and 48/49, respectively. Throughout the entire investigation, there was a significant correlation found in the simulation setup. The suggested antenna has demonstrated desirable measured -6 dB impedance bandwidths of 750 MHz. It can be demonstrated that the magnitude of isolation has a value of less than -10.03 dB throughout all the working bands of various

Preprints (www.preprints.org) | NOT PEER-REVIEWED | Posted: 29 August 2023 doi:10.20944/preprints202306.0073.v2

antenna pairs. Figure 6 illustrates the simulated coupling isolation between different antennas of a designed prototype, which is much lower than -10.03 dB, which is a good consideration. This demonstrates that our suggested design's coupling isolation between the antennas is better to demonstrate for future applications.

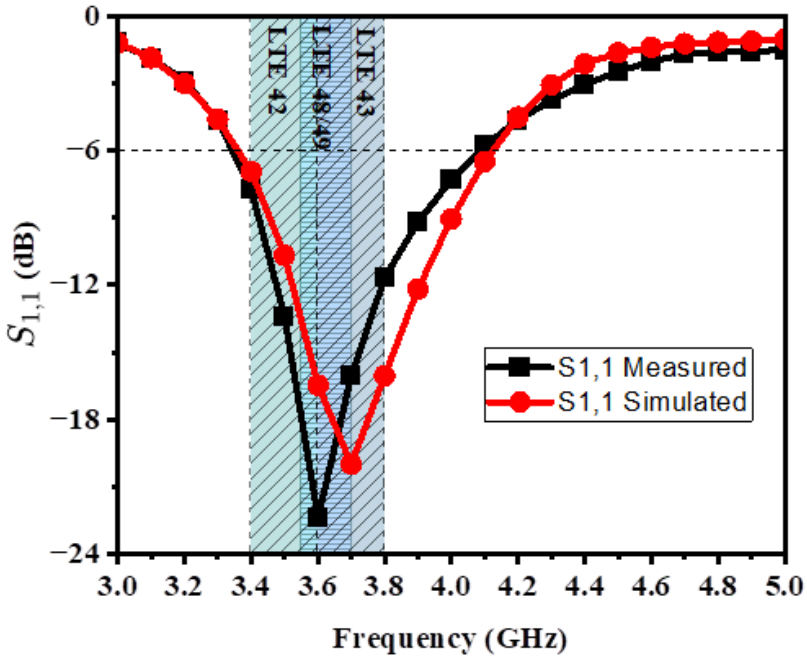

Figure 4. Measured reflection coefficient $S_{1,1}$ of antenna 1.

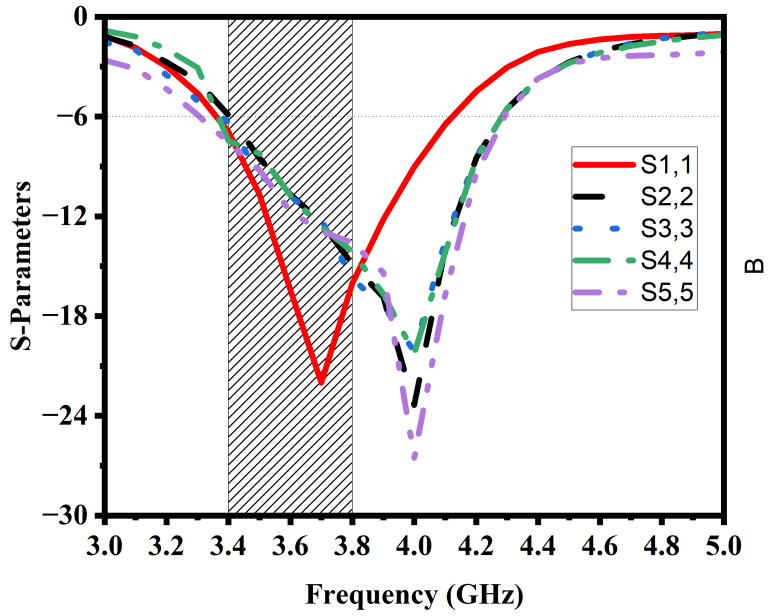

Figure 5. Simulated reflection coefficients of Ant 1 to Ant 5.

Preprints (www.preprints.org) | NOT PEER-REVIEWED | Posted: 29 August 2023 doi:10.20944/preprints202306.0073.v2

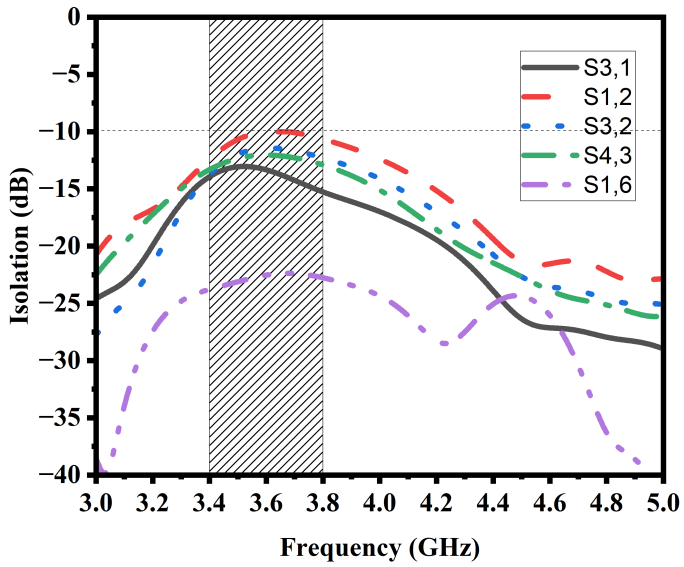

Figure 6. Simulated transmission coefficients (coupling) between different antenna pairs.

3.2. Diversity Gain and Envelop Correlation Coefficient

Investigating the diversity and multiplexing performances is crucial since, in addition to reflection, isolation, and radiation performances, diversity and multiplexing applications are the principal uses for the MIMO antenna. This section investigates the envelope correlation coefficients (ECCs) of various antenna pairs to assess and validate the diversity performance of the proposed MIMO antenna array [30]. The precise algorithm used to calculate the ECC has been made clear in [31]. Figure 7 demonstrates the proposed MIMO antenna's simulated diversity gain.

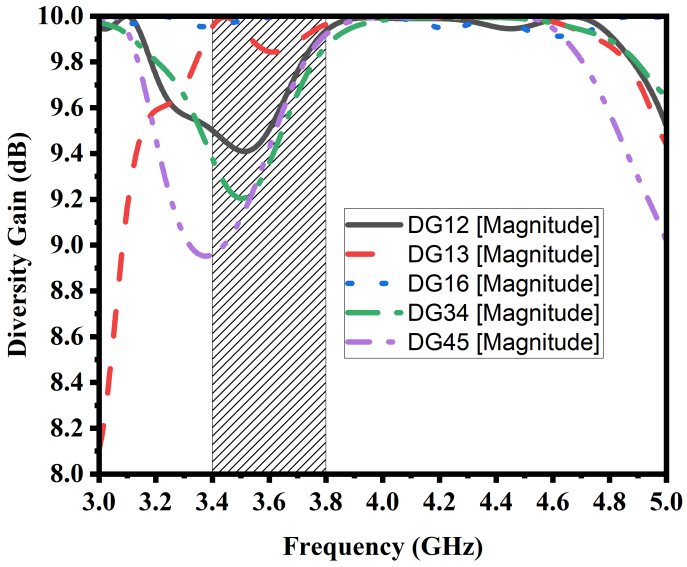

Figure 7. Simulated Diversity Gain of proposed antenna

Preprints (www.preprints.org) | NOT PEER-REVIEWED | Posted: 29 August 2023 doi:10.20944/preprints202306.0073.v2

Figure 8 shows the simulated ECC of the proposed antenna. The proposed MIMO antenna's ECC was determined using the data from the S-parameters. It can be seen in figure 8 that the calculated ECC values in LTE bands 42, 43, and 48/49 were less than 0.19, which is significantly better than the required ECC value of less than 0.25. The proposed MIMO antenna array has desirable diversity capabilities since lower ECC values will result in higher diversity gain.

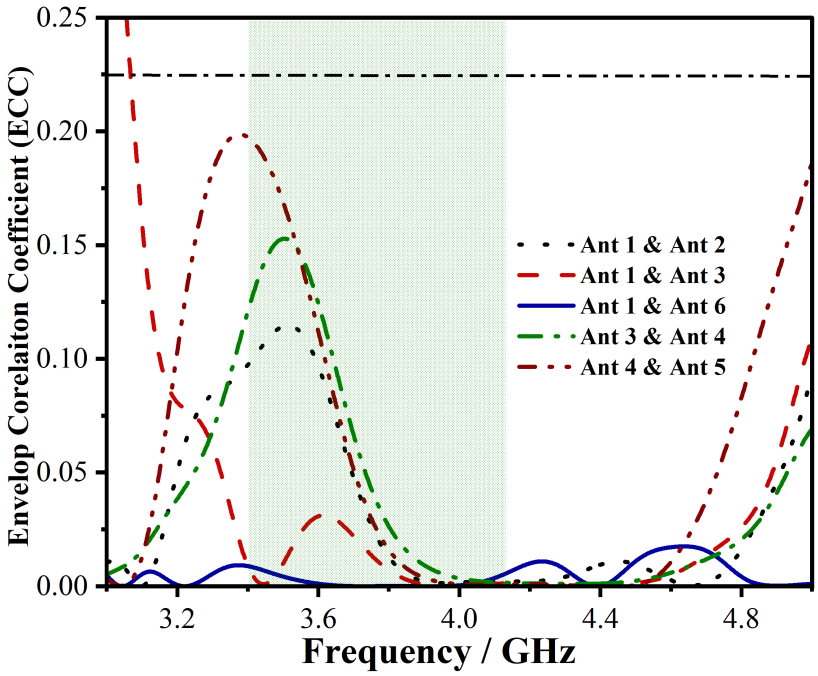

Figure 8. Calculated values for the envelope correlation coefficient (ECC) based on simulated s-parameters in the LTE bands 42, 43, and 48/49.

3.3. Gain of an Antenna and Current Distribution

Figure 9 shows the simulated and measured gain of a single element of the proposed 5G MIMO antenna array. The minimum and maximum simulated gain of the proposed 5G MIMO antenna is 1.8 dBi and 5.09 dBi which covers the necessary LTE bands 42, 43, and 48/49 bands, respectively. However, the maximum and minimum values of measured gain 4.8 dBi and 1.9 dBi are suitable for the suggested design and cover the necessary bands.

Figure 10 shows the current distribution of a proposed antenna, there is a maximum charge density due to the slot in the ground which is a necessary part to achieve the desired frequency band for LTE 42, 43, and 48/49.

Preprints (www.preprints.org) | NOT PEER-REVIEWED | Posted: 29 August 2023 doi:10.20944/preprints202306.0073.v2

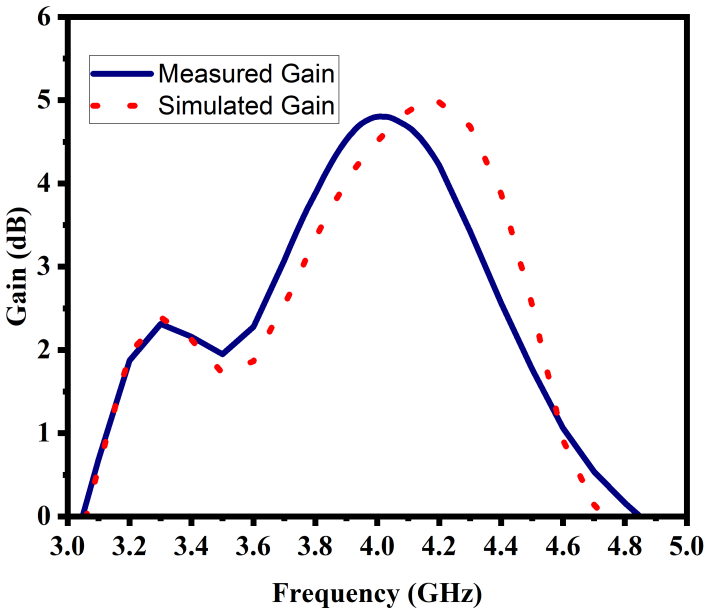

Figure 9. Simulated and Measured Gain of a Single Element

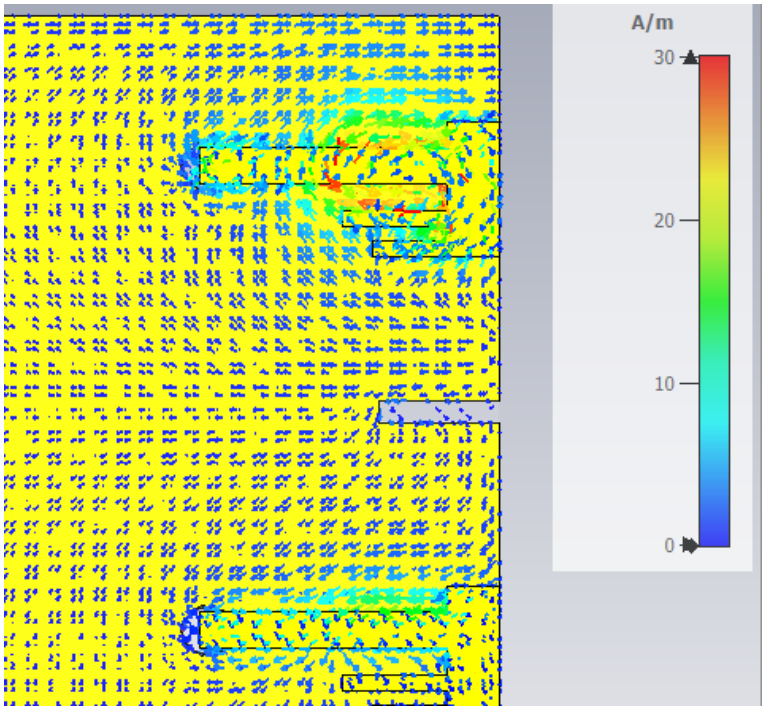

Figure 10. Current distribution of a proposed antenna at resonance

3.4. Radiation Pattern, Measurement Setup, and Comparison Table

The radiation pattern is the performance matric of an antenna that shows the power distribution in a 3D pattern. There are 10 antennas on a proposed PCB prototype with a similar shape but have a different pattern of each antenna, it is due to the current distribution effect of the adjacent antenna. Figure 11 (a) to (e), shows the e and h plane cuts off the 3D pattern of the first 5 antennas on the right

Preprints (www.preprints.org) | NOT PEER-REVIEWED | Posted: 29 August 2023 doi:10.20944/preprints202306.0073.v2

side from Figure 3 in simulated and measured scenarios. Similarly, Figure 11 (f) to (j), shows the e and h plane cuts off the 3D pattern of the other 5 antennas on the left side from Figure 3 in both simulated and measured scenarios. Figure 11 shows that there is approximately no difference in the h plane, but the e plane is inverted of opposite antennas.

Figure 12 is taken from the anechoic chamber while measuring the antenna gain and radiation pattern, the antenna is mounted on the turn table to move the antenna at 360-degree elevation and 180-degree azimuth, and the wide-band horn antenna is used as a receiver. the proposed 10 port massive MIMO antenna array is compared with some renowned articles in table 3. The fractional bandwidth is 19.9%, the ECC is 0.19 that's quite better to show good isolation.

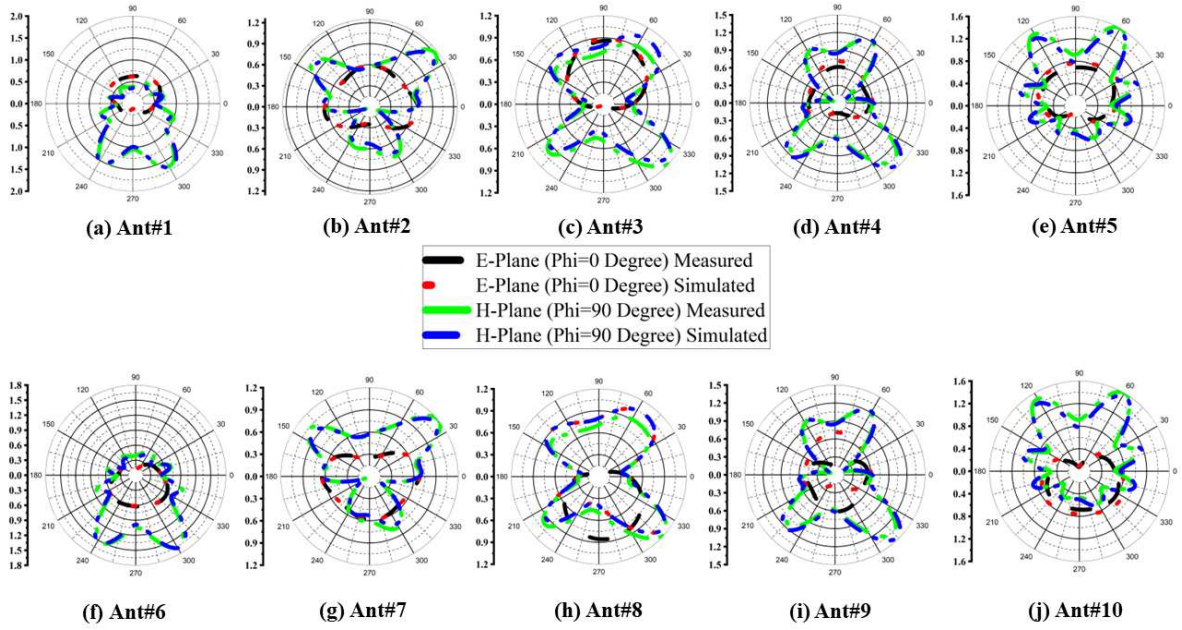

Figure 11. Measured and simulated radiation pattern of 10 port MIMO antenna array

Figure 12. Measurement Setup of a Proposed Antenna

Preprints (www.preprints.org) | NOT PEER-REVIEWED | Posted: 29 August 2023 doi:10.20944/preprints202306.0073.v2

Table 3. Performance comparison of various state-of-the-art 5G antennas.

Reference	Bandwidth (GHz)	Isolation (-dB)	ECC	Total Efficiency (%)	Radiator size in (λ^3)	Impedance Bandwidth (%)	Peak Channel Capacity (bps/Hz)
[Proposed]	3.4-3.6, 3.6-3.8 (-6dB)	>10	<0.19	>67	0.17 × 0.05 × 0.01	19.9	45 (10 × 10)
[32]	3.4-3.6, 5.15-5.92 (-6dB)	>12	<0.1	>50	0.17 × 0.05 × 0.01	19.71	38.8 (8 × 8)
[33]	3.4-3.6, 4.8-5.1 (-6dB)	>12	<0.1	40-85	0.17 × 0.03 × 0.01	11.77	38.5 (8 × 8)
[34]	2.49-2.69, 3.4-3.8 (-6dB)	>10.5	<0.2	44-66	0.02 × 0.17 × 0.01	18.59	38.3 (8 × 8)
[35]	3.35-3.82, 4.79-6.2 (-6dB)	>10.5	<0.12	>43	0.17 × 0.03 × 0.01	41.77	37.6 (8 × 8)
[36]	3.4-3.8, 5.15-5.92 (-6dB)	>12	<0.15	41-79	0.13 × 0.04 × 0.01	25.11	29.5 (6 × 6)
[37]	3.4-3.6, 3.6-3.8 (-10dB)	>20	<0.01	>87	0.11 × 0.04 × 0.02	11.11	81 (18 × 18)
[38]	3.4-3.6, 4.8-5 (-10dB)	>16.5	<0.01	82-85	0.16 × 0.07 × 0.01	9.79	Not Mentioned (4 × 4)
[39]	3.3-3.8, 4.8-5, 5.15-5.35, 5.72-5.85 (-10dB)	>15	<0.02	>70	0.16 × 0.07 × 0.01	24.02	Not Mentioned (4 × 4)
[40]	3.1-3.85, 4.8-6 (-10dB)	>17	<0.06	65-71	0.20 × 0.05 × 0.01	36.17	39 (8 × 8)
[41]	3.3-4.2, 4.8-5.0 (-6dB)	>10	<0.12	53.8-79.1	0.21 × 0.07 × 0.01	28.10	39.5 (8 × 8)
[42]	2-2.4, 5.8-6.1 (-6dB)	>48	<0.12	70-84	0.24 × 0.108 × 0.001	15.38	39.5 (12 × 12)

4. Conclusion

The main target of this article is to design a 5G massive MIMO antenna array that can provide a high gain, high efficiency, and a minimum coefficient of correlation joining the antenna section. The suggested antenna array is anticipated to raise data rates, increase channel capacity, and improve signal quality in order to fulfill the needs of 5G wireless networks. The radiation pattern, gain, efficiency, and correlation coefficient are used to assess how well the planned antenna array performs. According to the simulation results, the suggested antenna array has a low correlation coefficient between the antenna elements, a peak diversity gain of 9.5 dBi, and a total efficiency of 67 %. In conclusion, the suggested 10-element 5G massive MIMO antenna array is a potential option for mobile devices

 doi:10.20944/preprints202306.0073.v2

operating below 6 GHz, especially for LTE bands 42/43/48/49 applications. The system capacity and spectral efficiency of 5G wireless networks can both be greatly increased by the suggested antenna array. The proposed prototype is compared with some MIMO antennas for smartphones literature in Table 2.

References

1. Abubaker Ahmed Elobied, Xue-Xia Yang, Ningjie Xie, Steven Gao, "Dual-Band 2×2 MIMO Antenna with Compact Size and High Isolation Based on Half-Mode SIW", International Journal of Antennas and Propagation, vol. 2020, Article ID 2965767, 11 pages, 2020.
2. S. Zhang, K. Zhao, Z. Ying and S. He, "Adaptive Quad-Element Multi-Wideband Antenna Array for User-Effective LTE MIMO Mobile Terminals," in IEEE Transactions on Antennas and Propagation, vol. 61, no. 8, pp. 4275-4283, Aug. 2013, doi: 10.1109/TAP.2013.2260714.
3. Liu, X., Zhang, J., Xi, H., Yang, X., Sun, L. and Gan, L., 2022. A Compact Four-band High-isolation Quad-port MIMO Antenna for 5G and WLAN Applications. AEU-International Journal of Electronics and Communications, p.154294.
4. Elfergani, I., Hussaini, A. S., Abd-Alhameed, R., See, C., Child, M., & Rodriguez, J. (2012). Design of a compact tuned antenna system for mobile MIMO applications
5. J. Dong, S. Wang, and J. Mo, "Design of a Twelve-Port MIMO Antenna System for Multi- Mode 4G/5G Smartphone Applications Based on Characteristic Mode Analysis," in IEEE Access, vol. 8, pp. 90751-90759, 2020, doi: 10.1109/ACCESS.2020.2994068.
6. Z. Li, Z. Du, M. Takahashi, K. Saito, and K. Ito, "Reducing mutual coupling of MIMO antennas with parasitic elements for mobile terminals," IEEE Trans. Antennas Propag., vol. 60, no. 2, pp. 473–481, Feb. 2012.
7. Li, M., Jiang, L. & Yeung, K. L. A general and systematic method to design neutralization lines for isolation enhancement in MIMO antenna arrays. IEEE Trans. Vehicular Technol. (2020).
8. M. Ikram, M. S. Sharawi, A. Shamim, and A. Sebak, "A multiband dual standard MIMO antenna system based on monopoles (4G) and connected slots (5G) for future smart phones," Microw. Opt. Technol. Lett., vol. 60, no. 6, pp. 1468–1476, Jun. 2018.
9. Q. Sun, B. Sun, L. Sun, W. Huang, and Q. Ren, "Broadband two-element array with hybrid decoupling structures for multimode mobile terminals," IEEE Antennas Wireless Propag. Lett., vol. 14, pp. 1431–1434, 2015.
10. J. Dong, X. Yu, and L. Deng, "A decoupled multiband dual-antenna system for WWAN/LTE smartphone applications," IEEE Antennas Wireless Propag. Lett., vol. 16, pp. 1528–1532, 2017.
11. K. Yu, Y. Li, and X. Liu, "Mutual coupling reduction of a MIMO antenna array using 3D novel meta material structures," Appl. Comput. Electromagn. Soc. J., vol. 33, no. 7, pp. 758–763, 2018.
12. M.-Y. Li, Y.-L. Ban, Z.-Q. Xu, J. Guo, and Z.-F. Yu, "Tri-polarized 12-antenna MIMO array for future 5G smartphone applications," IEEE Access, vol. 6, pp. 6160–6170, 2018.
13. Zhu, F.-G., Xu, J.-D. & Xu, Q. Reduction of mutual coupling between closely-packed antenna elements using defected ground structure. Electron. Lett. 45, 601–602 (2012).
14. Suntives, A. & Abhari, R. Miniaturization and isolation improvement of a multiple-patch antenna system using electromagnetic bandgap structures. Microw. Opt. Technol. Lett. 55, 1609–1612 (2013).
15. Adamiuk, G., Beer, S., Wiesbeck, W. & Zwick, T. Dual-orthogonal polarized antenna for UWB-IR technology. IEEE Antennas Wireless Propag. Lett. 8, 981–984 (2009).
16. Iqbal, A., Saraereh, O. A., Ahmad, A. W. & Bashir, S. "Mutual coupling reduction using F-shaped stubs in UWB-MIMO antenna." IEEE Access. 6, 2755–22759 (2017).
17. Pandit, S., Mohan, A., Ray, P. A compact planar MIMO monopole antenna with reduced mutual coupling for WLAN applications using ELC resonator. in Proc. IEEE Microw. Conf. (APMC), pp. 1–4 (2016).
18. Verma, A.K., Nakkeeran, R., Vardhan, R.K. Design of 2x2 single-sided wrench-shaped UWB MIMO antenna with high isolation. in Proc. IEEE Int. Conf. Circuit, Power Comput. Technol. (ICCPCT), pp. 1–3 (2016).
19. Cui, L., J. Guo, Y. Liu, and C. Sim, "An 8-element dual-band MIMO antenna with decoupling stub for 5G smartphone applications," IEEE Antennas and Wireless Propagation Letters, Vol. 18, No. 10, 2095–2099, Oct. 2019.

20. Li, Y., C. Sim, Y. Luo, and G. Yang, "High isolation 3.5 GHz eight antenna MIMO array using balanced open-slot antenna element for 5G smartphones," IEEE Transactions on Antenna and Propagation, Vol. 67, No. 6, 3820–3830, 2019.
21. Andrews Christina Malathi and Dhanasingh Thiripurasundari, "Compact 2×1 MIMO Antenna System for LTE Band," Progress In Electromagnetics Research C, Vol. 75, 63-73, 2017.
22. F. Alexa, B. Bardeanu and D. Vatau, "MIMO antenna system for LTE," 2013 36th International Conference on Telecommunications and Signal Processing (TSP), Rome, Italy, 2013, pp. 294-298, doi: 10.1109/TSP.2013.6613939.
23. Qualcomm. (Sep. 2015). Making the Best Use of Licensed and Unlicensed Spectrum. [Online]. Available: https://www.qualcomm.com/media/documents/files/making-the-best-use-of-unlicensed-spectrum presentation.pdf
24. IMT-2020 (5G) Promotion Group. (Feb. 2015). White Paper on 5G Concept. [Online]. Available: http://www.imt-2020.org.cn/zh/ documents/download/4
25. SK Telecom. (Oct. 2014).SK Telecom 5G White Paper.[Online]. Available:http://www.sktelecom.com/img/pds/press/SKT-5G%20White%20Paper_V1.0_Eng.pdf.
26. M. Arunraj, A. Mathivadhani, D. Deepa and S. A. Kumar, "Design of F shaped MIMO antenna for WIMAX Applications," 2019 Third International Conference on Inventive Systems and Control (ICISC), Coimbatore, India, 2019, pp. 159-161, doi: 10.1109/ICISC44355.2019.9036364.
27. X. -T. Yuan, Z. Chen, T. Gu and T. Yuan, "A Wideband PIFA-Pair-Based MIMO Antenna for 5G Smartphones," in IEEE Antennas and Wireless Propagation Letters, vol. 20, no. 3, pp. 371-375, March 2021, doi: 10.1109/LAWP.2021.3050337.
28. D. Rajesh Kumar, G. V. Babu and K. G. S. Narayan, "Compact F-Shaped Antenna with its Analytical Modelling Resonating at 3.5 GHz for 5G Applications," 2021 IEEE Indian Conference on Antennas and Propagation (InCAP), Jaipur, Rajasthan, India, India, 2021, pp. 01-04, doi: 10.1109/InCAP52216.2021.9726421.
29. N. O. Parchin et al., "Modified PIFA Array Design with Improved Bandwidth and Isolation for 5G Mobile Handsets," 2019 IEEE 2nd 5G World Forum (5GWF), Dresden, Germany, 2019, pp. 199-203, doi: 10.1109/5GWF.2019.8911725.
30. M. S. Sharawi, "Printed Multi-Band MIMO Antenna Systems and Their Performance Metrics [Wireless Corner]," in IEEE Antennas and Propagation Magazine, vol. 55, no. 5, pp. 218-232, Oct. 2013, doi: 10.1109/MAP.2013.6735522.
31. Y. Li, C. -Y. -D. Sim, Y. Luo and G. Yang, "12-Port 5G Massive MIMO Antenna Array in Sub-6GHz Mobile Handset for LTE Bands 42/43/46 Applications," in IEEE Access, vol. 6, pp. 344-354, 2018, doi: 10.1109/ACCESS.2017.2763161.
32. H. Zou, Y. Li, C.-Y.-D. Sim, and G. Yang, "Design of 8 × 8 dual-band MIMO antenna array for 5G smartphone applications," Int. J. RF Microw. Comput.-Aided Eng., vol. 28, no. 9, p. e21420, 2018.
33. J. L. Guo, L. Cui, C. Li, and B. H. Sun, "Side-edge frame printed eight-port dual-band antenna array for 5G smartphone applications," IEEE Trans. Antennas Propag., vol. 66, no. 12, pp. 7412–7417, Dec. 2018.
34. Y. Li, C.-Y.-D. Sim, Y. Luo, and G. Yang, "Metal-frame-integrated eight-element multiple-input multiple-output antenna array in the long term evolution bands 41/42/43 for fifth generation smartphones," Int. J. RF Microw. Comput.-Aided Eng., vol. 29, no. 1, Jan. 2019, Art. no. e21495.
35. H. Wang, R. Zhang, Y. Luo, and G. Yang, "Compact eight-element antenna array for triple-band MIMO operation in 5G mobile terminals," IEEE Access, vol. 8, pp. 19433–19449, 2020.
36. Y. Li, C.-Y.-D. Sim, Y. Luo, and G. Yang, "12-port 5G massive MIMO antenna array in sub-6 GHz mobile handset for LTE bands 42/43/46 applications," IEEE Access, vol. 6, pp. 344–354, Oct. 2017.
37. N. Jaglan, S. D. Gupta, and M. S. Sharawi, "18 element massive MIMO/diversity 5G smartphones antenna design for sub-6 GHz LTE bands 42/43 applications," IEEE Open J. Antennas Propag., vol. 2, pp. 533–545, 2021.
38. J. Huang, G. Dong, J. Cai, H. Li, and G. Liu, "A quad-port dualband MIMO antenna array for 5G smartphone applications," Electronics, vol. 10, no. 5, p. 542, Feb. 2021.
39. J. Huang, G. Dong, Q. Cai, Z. Chen, L. Li, and G. Liu, "Dual-band MIMO antenna for 5G/WLAN mobile terminals," Micromachines, vol. 12, no. 5, p. 489, Apr. 2021.
40. D. Serghiou, M. Khalily, V. Singh, A. Araghi, and R. Tafazolli, "Sub-6 GHz dual-band 8 × 8 MIMO antenna for 5G smartphones," IEEE Antennas Wireless Propag. Lett., vol. 19, no. 9, pp. 1546–1550, Sep. 2020.

41. L. Cui, J. Guo, Y. Liu, and C.-Y.-D. Sim, “An 8-element dual-band MIMO antenna with decoupling stub for 5G smartphone applications,” IEEE Antennas Wireless Propag. Lett., vol. 18, no. 10, pp. 2095–2099, Oct. 2019.
42. M. Ahmed, Z. Zafar, I. Javed, M. Zahid and Y. Amin, "12 Element Inverted E-Shaped Massive MIMO Antennas for Future 5G Smartphone Applications," 2023 7th International Multi-Topic ICT Conference (IMTIC), Jamshoro, Pakistan, 2023, pp. 1-5, doi: 10.1109/IMTIC58887.2023.10178604.